

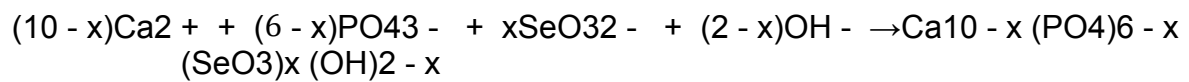
## Supporting Information

**Platinum-loaded, selenium-doped hydroxyapatite nanoparticles selectively reduce proliferation of prostate and breast cancer cells co-cultured in the presence of stem cells.**

Alessandra Barbanente, Robin A. Nadar, Lorenzo Degli Esposti, Barbara Palazzo, Michele Iafisco, Jeroen J. J. P. van den Beucken, Sander C. G. Leeuwenburgh, and Nicola Margiotta.

**Equation 1** Description of the incorporation of Se anions into the apatitic lattice.

The substitution of a divalent Se anion for a trivalent orthophosphate anion creates a positively charged vacancy (+1). This charge defect is compensated by one calcium cation vacancy and one hydroxyl anion vacancy. As a consequence, we can observe a simultaneous decalcification and dehydroxylation in the apatite sample. In order to comply with the aforementioned formula, the amounts of reagents were calculated assuming that one orthophosphate ion and one calcium ion are replaced by one Se ion.



(eqn (1))

### **IR Characterization of HAsSe nanoparticles.**

The characteristic hydroxyapatite bands were present in all spectra (Figure 1B). The dominant bands at around 1092 and 1037  $\text{cm}^{-1}$ , as well as the bands at 603 and 567  $\text{cm}^{-1}$ , correspond to the vibrations of the phosphate ( $\text{PO}_4^{3-}$ ) groups of hydroxyapatite. The intensity of the infrared  $\text{PO}_4^{3-}$  stretching bands (1037  $\text{cm}^{-1}$  with its shoulder at 1092  $\text{cm}^{-1}$ ) intensity decreased with increasing Se substitution. Moreover, additional peaks were detected at 770  $\text{cm}^{-1}$  and in the range between 830 and 870  $\text{cm}^{-1}$ , which can be assigned to Se-O vibrations of the selenite ions in HA nanoparticles. Selenite absorptions were detected at 740, 790, 840 and 880  $\text{cm}^{-1}$ . Incorporation of selenite ions into HA nanoparticles resulted in shifting of the bands to lower/higher wavenumbers with increasing selenite substitution percentage. In the spectra of HAsSe1% only a band around 870  $\text{cm}^{-1}$  was detected. The spectra of HAsSe10% and HAsSe25% presented a band at around 765  $\text{cm}^{-1}$  with a shoulder at about 820  $\text{cm}^{-1}$  and a band at 846  $\text{cm}^{-1}$ . A general shifting of the band to lower wavenumbers was observed, which was attributed to a change in the counter ions surrounding incorporated selenite with respect to sodium selenite.

**Figure S1.** Schematic representation for synthesis of HAsE nanoparticles and Pt-loaded HAsE nanoparticles.

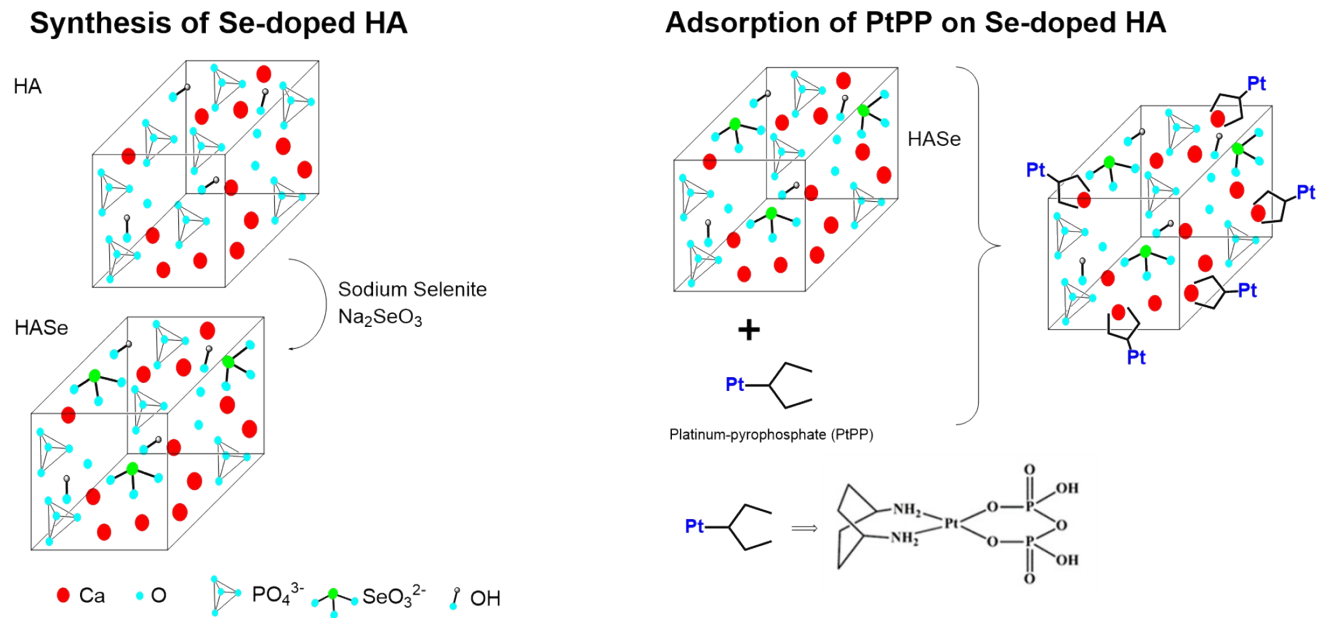


**Figure S2.** Dose-response curves for prostate cancer, breast cancer and bone marrow stem cells treated with sodium selenite ( $\text{Na}_2\text{SeO}_3$ ) measured using (A) CCK-8 assay and (B) DNA assay. Dose-response curves for prostate cancer, breast cancer and bone marrow stem cells treated with PtPP measured using (C) CCK-8 assay and (D) DNA assay. Cell viability is plotted against the logarithm of Pt concentrations.

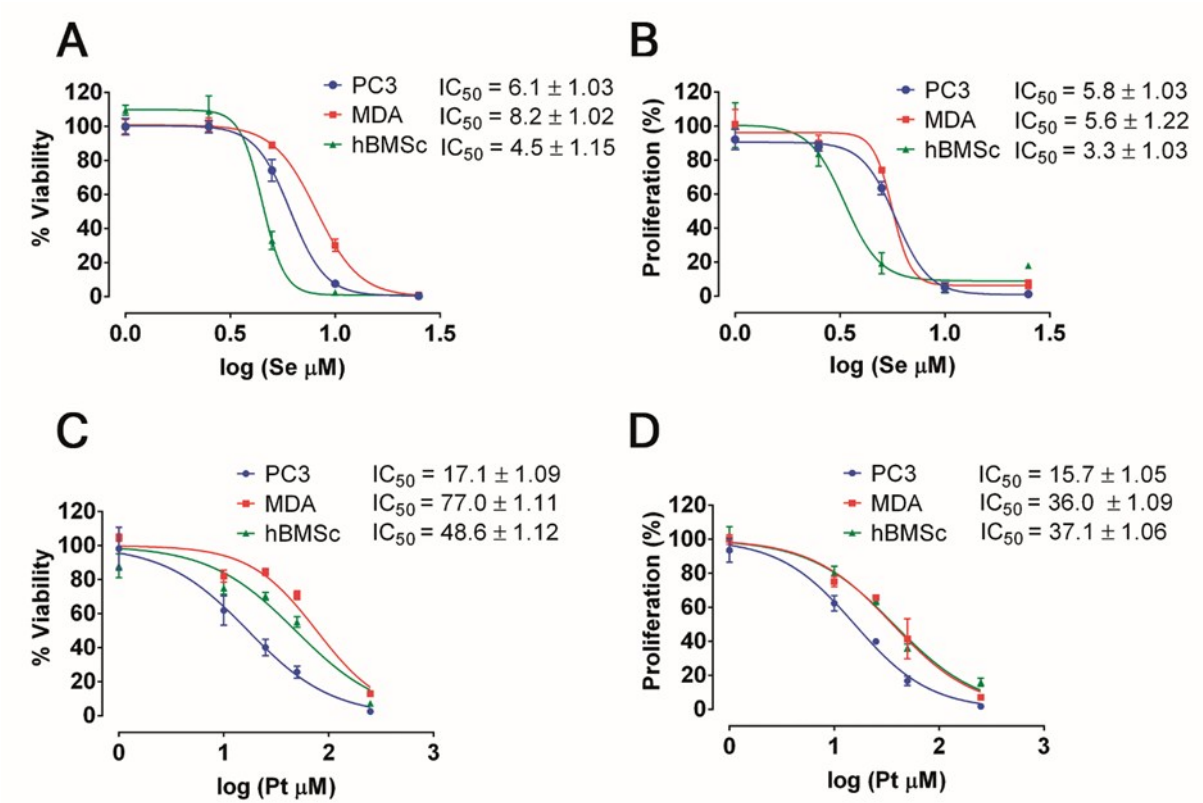


**Figure S3.** In vitro effects of Pt or Se releasates from Pt-loaded or HAsE. The cytotoxicity of Se releasates obtained at pH 7.4 on (A) viability and (B) proliferation of prostate cancer, breast cancer and bone marrow stem cells. The cytotoxicity of Se releasates obtained at pH 6.5 on (C) viability and (D) proliferation of prostate cancer, breast cancer and bone marrow stem cells. The cytotoxicity of Pt releasates obtained at pH 7.4 on (E) viability and (F) proliferation of prostate cancer, breast cancer and bone marrow stem cells. The cytotoxicity of Pt releasates obtained at pH 6.5 on (G) viability and (H) proliferation of prostate cancer, breast cancer and bone marrow stem cells. \*P < 0.05; \*\*P < 0.01; \*\*\*P < 0.001; \*\*\*\*P < 0.0001.

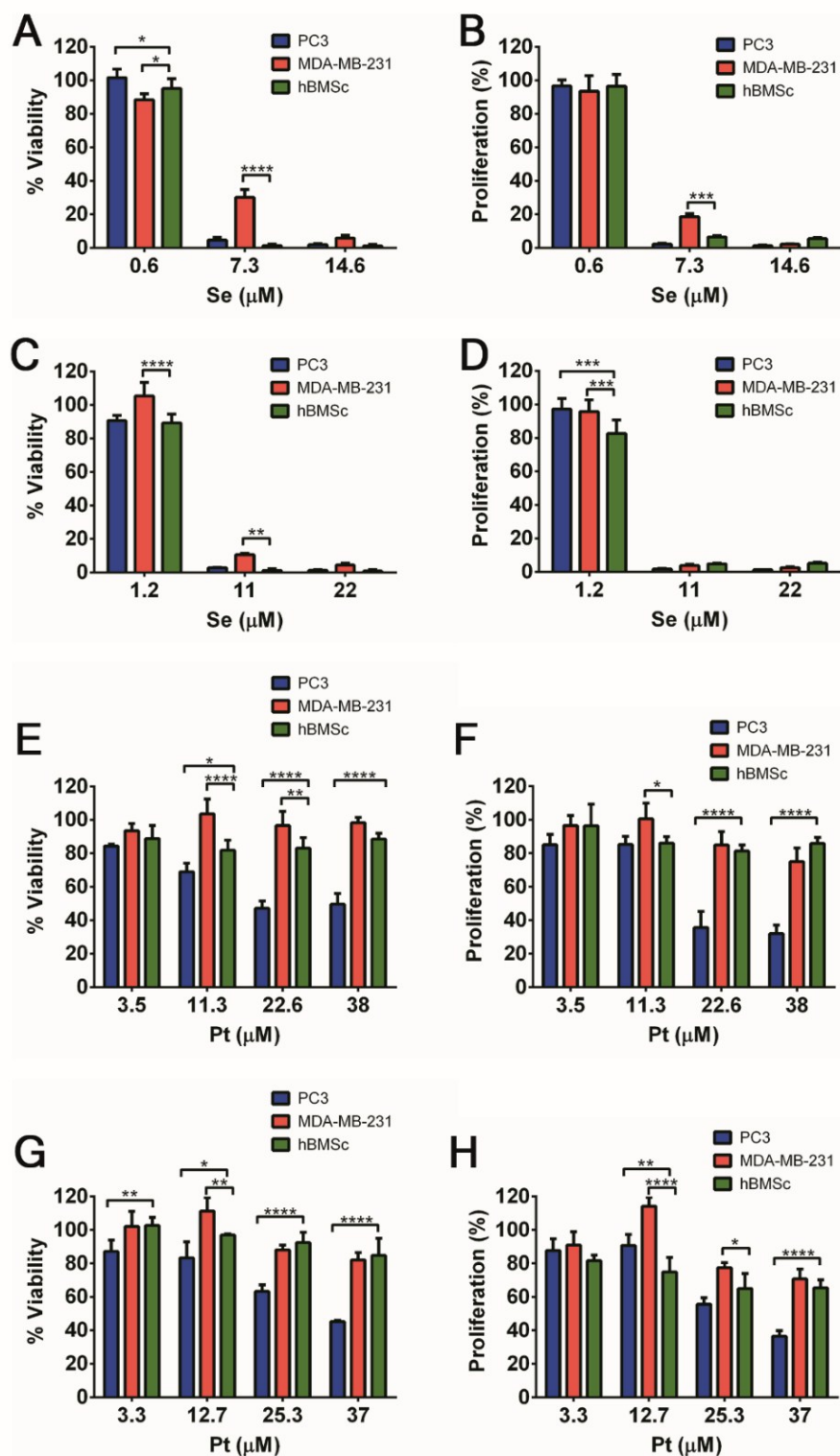


**Figure S4.** Viability and proliferation of prostate cancer, breast cancer and bone marrow stem cells treated with fixed concentration of 10  $\mu\text{M}$   $\text{Na}_2\text{SeO}_3$  and increasing concentration of Pt drugs resulting in Pt/Se ratios between 0 and 8. (A, B) Viability and proliferation of prostate cancer, breast cancer and bone marrow stem cells treated with combination of PtPP and  $\text{Na}_2\text{SeO}_3$ . (C, D) Viability and proliferation of prostate cancer, breast cancer and bone marrow stem cells treated with combination of kiteplatin and  $\text{Na}_2\text{SeO}_3$ . (E, F) Viability and proliferation of prostate cancer, breast cancer and bone marrow stem cells treated with combination of cisplatin and  $\text{Na}_2\text{SeO}_3$ . \*\*0.001 <P < 0.01; \*\*\*0.0001 <P < 0.001; \*\*\*\*P <0.0001. The labels for prostate cancer (PC3, blue), breast cancer (MDA-MB-231, red), and bone marrow stem (hBMSc, green) cells are the same in A—F and are reported in the upright corner of the figure.

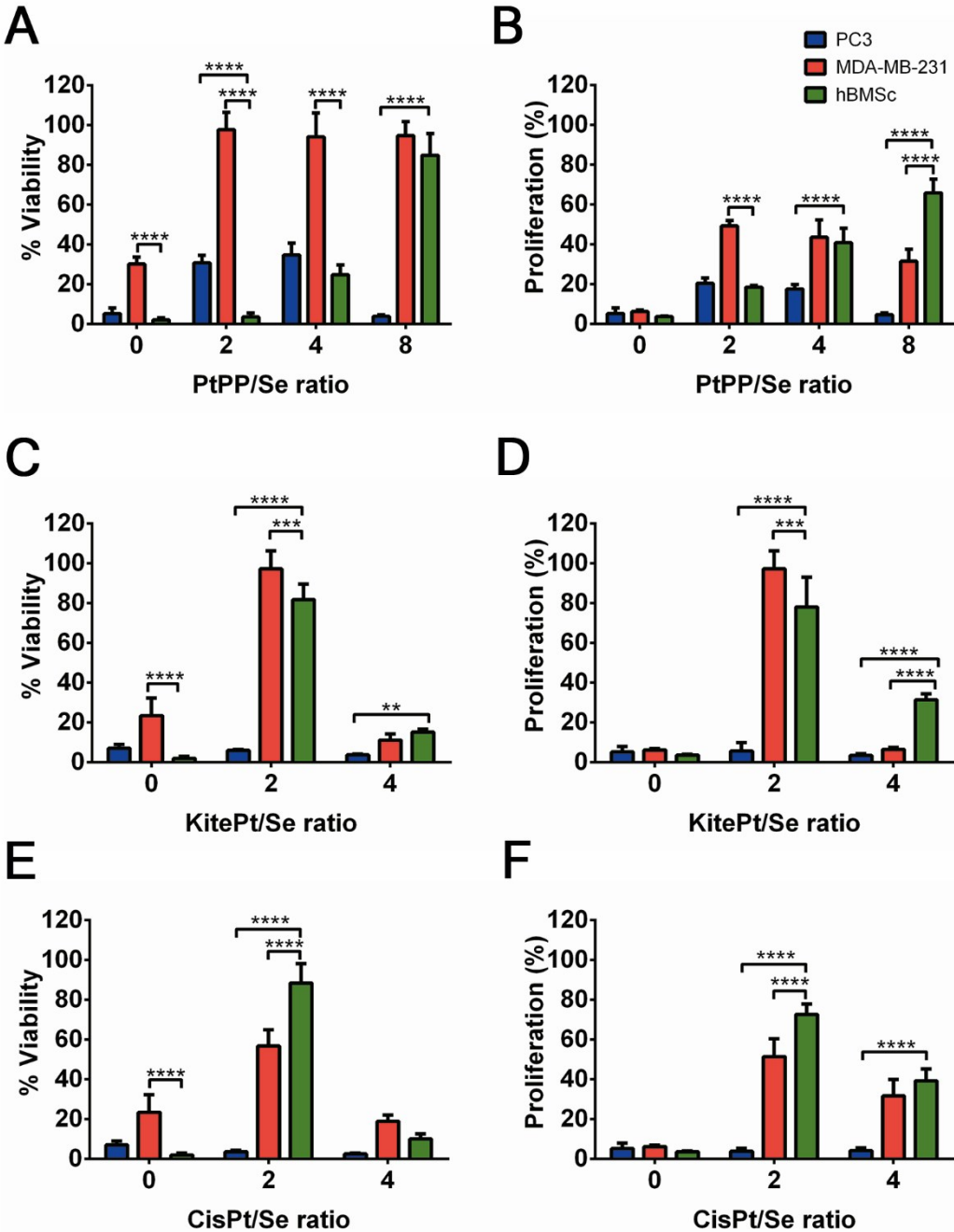


**Figure S5.** Dose-response curves for prostate cancer, breast cancer and bone marrow stem cells treated with kiteplatin measured using (A) CCK-8 assay and (B) proliferation assay.

